Thermal mixing enhancement of liquid metal MHD free-surface flow by optimizing vortex generator arrays

Koji Kusumi[a], Tomoaki Kunugi[a,*], Takehiko Yokomine[a], Zensaku Kawara[a], Shoki Nakamura[a], Egemen Kolemen[b], Hantao Ji[b]

[a] Department of Nuclear Engineering, Kyoto University, C3-d2S06, Kyoto, 615-8540, Japan
[b] Princeton Plasma Physics Laboratory, 100 Stellarator Road, Princeton, New Jersey 08540, USA

ABSTRACT

Liquid divertor concepts in fusion reactor research have been widely studied. Recently, thermal mixing enhancement of the locally heated free-surface of liquid metal MHD (Magneto-Hydro-Dynamics) film flow using one vortex generator was proposed and investigated by the authors. In this study, an inline arrangement of many hemispherical protrusions to generate many vortices in their wakes was proposed, and the transport characteristics of high temperature fluid at the free-surface to the bottom (i.e., thermal mixing) in liquid metal MHD film flow was investigated experimentally. The experiments for three streamwise pitch lengths between the protrusions under various transverse magnetic field strengths (B = 0.00–0.33T) for two flowrate conditions were conducted. As the results, the heat flux distributions on the bottom wall of the film flow and the efficiency of heat transport showed the existence of the optimum streamwise pitch length for the thermal mixing enhancement even under relatively high transverse magnetic field. Therefore, the inline arrangement of many hemispherical protrusions can be considered as one of the candidates for thermal mixing enhancement methods of liquid metal MHD free-surface flow application.

1. Introduction

There are many heat transfer enhancement techniques applied to heat exchangers and nuclear reactor fuel rods such as ribs, fins and turbulence promoters [1–4]. However, the effect of these protrusions on heat transfer enhancement of the liquid metal MHD (Magneto-Hydro-Dynamics) film flow has been studied a little. Rhoads [5] investigated the effect of the magnetic field on heat transfer performance of liquid metal film flow with heating locally on the free surface under the vertical magnetic field. He reported that the MHD flow under the vertical magnetic field showed better performance for heat transfer enhancement than the case of the transverse magnetic field. The Regarding the thermal mixing characteristics of the liquid metal MHD film flow with locally heated on the free-surface assuming the application to a divertor of nuclear fusion reactors, there is no study except a delta wing vortex generator by the authors [6,7].

In our previous studies [6,7], the thermal mixing characteristics of liquid metal film flow with locally heated free-surface without magnetic field was studied in the case of installing a delta wing, and its heat transport performance showed higher than both that of flat plate and a cubic. It was confirmed that the delta-wing obstacle generated a strong

suction flow from the free-surface to the bottom wall caused by a pair of vortex having the vortex axis parallel to the flow direction, and this suction flow caused the enhancement of a thermal mixing. In case of the transverse magnetic field applied, the heat transport efficiency was also higher in case of installing the delta-wing in the liquid metal film flow than that of the flat plate. Moreover, it was found that the strength of a pair of vortex generated from the delta wing decreased with increase of the magnetic field strength, and the heat transport efficiency decreased too.

To know the thermal mixing characteristics and the optimum arrangement of the protrusions are very important to apply this protrusion method to enhance the thermal mixing in the divertor design. Thus, the optimum arrangement of the protrusion array should be investigated. There are two arrangements of the protrusions: the inline arrangement and a staggered arrangement. In this study, the inline arrangement was focused, for the simplicity, and the arrangements for the various streamwise pitch length with a constant spanwise pitch length using the hemispherical protrusions were experimentally investigated. Resulting, it was found the optimal length as the streamwise pitch length, and it clarified the influence of the transverse magnetic field strength and the geometrically optimum arrangement condition of
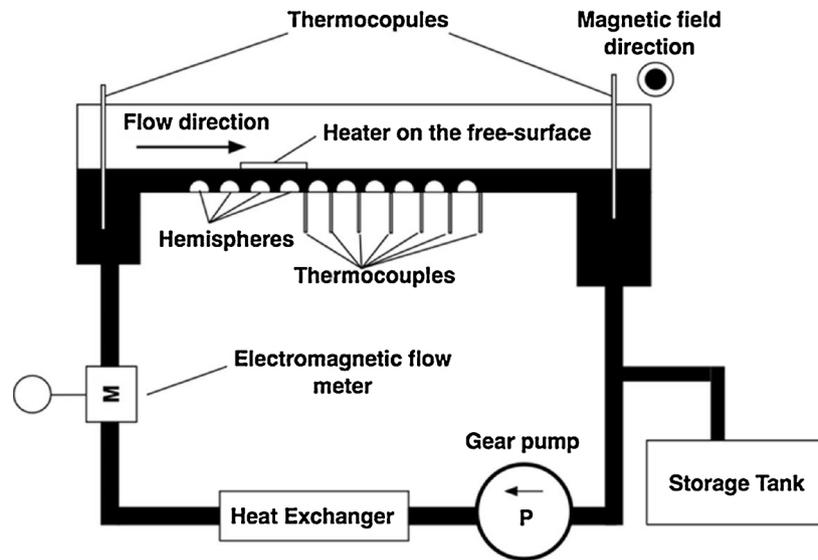

Fig. 1. Experimental apparatus (black area is working fluid; white area is injected argon gas).

the protrusion array. Finally, the problems and suggestions of the application to the divertor design were briefly discussed.

2. Experimental apparatus and conditions

The experimental apparatus used in this study is called the "LMX (Liquid Metal eXperiment)" at the Princeton Plasma Physics Laboratory (PPPL). The LMX consists of an acrylic channel whose length of l.08 m and the width of 0.10 m as a test section, an electromagnet flow meter, a mechanical gear pump, a heat exchanger cooled by 25.0 °C de-ionized water, a set of electromagnets (transverse magnetic field) and a storage tank as illustrated in Fig. 1. The working fluid was a gallium–indium–tin ($Ga_{67}In_{20.5}Sn_{12.5}$) eutectic alloy that flowed through the channel with the mean depth of 0.06×10^{-1}–0.11×10^{-1} m at the flow velocity of 0.10–0.16 ms^{-1}, the volumetric flow rate was kept constant in this experiment, so the depth naturally increased with increase of the magnetic field strength. Argon gas was used to prevent the oxidation of the liquid metal. 25 K-type TCs with an accuracy of ±

0.10 °C were installed on the bottom of the channel with mostly equal distance of 0.34×10^{-2} m as illustrated in Fig. 2. In order to evaluate the net heat flux by calculating the heat loss and the mean temperature gradient of the flow, K-type TCs were installed in the fluid at the inlet and outlet centers of the channel. The hemispherical protrusions arrays of the inline configuration is illustrated in Fig. 2, in which L_p is a streamwise pitch length: 1.75×10^{-2} mm, 0.36×10^{-1} m and 0.48×10^{-1} m. L_t is the distance from first TCs array: $L_t = 0.41 \times 10^{-2}$ m for $L_p = 1.75 \times 10^{-2}$ m, $L_t = 1.41 \times 10^{-3}$ m for $L_p = 0.36 \times 10^{-1}$ m and $L_t = 0.17 \times 10^{-1}$ m for $L_p = 0.48 \times 10^{-1}$ m. L_w is a spanwise pitch length of 1.95×10^{-2} m in all cases. The array of hemispheres of 8.00×10^{-1} m diameter were installed at the TCs area and at the upstream of TCs at least 10 rows or more. The blockage ratio of obstacle to the cross-section of the flow channel was roughly 0.37. The experiments were performed at the Reynolds number (Re = $U(L/2)/\nu$; where U[ms^{-1}] is mean velocity, L[m] is hydrodynamic diameter and ν[m^{2}s^{-1}] is kinematic viscosity) of $5.53 \times 10^3 <$ Re $< 6.38 \times 10^3$, and with the interaction parameter
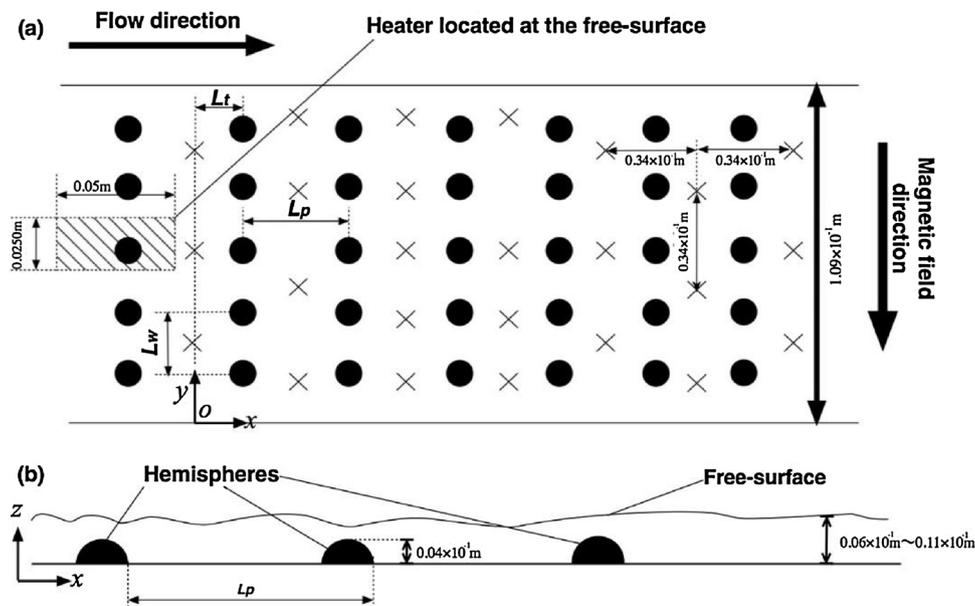

Fig. 2. Schematic of heater location, hemispheres locations and TCs mapping on channel bottom ("×"marks show TC locations, ● show hemispheres locations on bottom wall, *x, y* and *z* show the coordination, *o* is the origin of the coordination): (a) Top view of thermocouples area (b) Cross-sectional view of hemisphere arrangements.

Table 1
Experimental conditions in this study.

Experiment index	Flow rate $Q_{flowrate}[\text{m}^3\,\text{s}^{-1}]$	Streamwise pitch length $L_p[\text{m}]$	Interaction parameter N $[-]$
A	1.21×10^{-4}	1.75×10^{-2}	0.00–9.03
B	1.21×10^{-4}	0.36×10^{-1}	0.00–7.92
C	1.21×10^{-4}	0.48×10^{-1}	0.00–7.95
D	1.67×10^{-4}	1.75×10^{-2}	0.00–9.25
E	1.67×10^{-4}	0.36×10^{-1}	0.00–7.92
F	1.67×10^{-4}	0.48×10^{-1}	0.00–9.18

(Na = Ha^2/Re: where Ha is the Hartmann number which is defined as Ha = $B(L/2)\sqrt{\sigma/\rho\nu}$, where $B\,[\text{T}]$ is applied magnetic field strength, $\sigma\,[\text{AV}^{-1}\text{m}^{-1}]$ is fluid electrical conductivity, $\rho\,[\text{kgm}^{-3}]$ is fluid density) of $0.00 < \text{N} < 9.18$. The flow circulation was driven by a mechanical pump with the desired flow rate. The heater plate made of Aluminum Nitride ceramic (0.05 m length $\times\ 0.25 \times 10^{-1}$ m width) was used for locally heating on the free-surface. This heater supplied a constant heat flux of $0.14\,\text{MWm}^{-2}$ into the fluid, and raised the free-surface temperature by a few degrees. The heat exchanger installed after the pump was used to cool the heated fluid down to its initial temperature. The experimental conditions in this study are listed on Table 1.

3. Analysis

The temperatures were measured by TCs installed at the channel bottom wall and at the inlet and outlet of the channel. The bulk temperature $T_b\,[°\text{C}]$ was assumed to be linear as $T_b = (T_{out} - T_{in})x/L_{channel} + T_{in}$ where, $T_{out}\,[°\text{C}]$ is temperature at the outlet of the channel, $T_{in}\,[°\text{C}]$ is temperature at the inlet of the channel, $L_{channel}$ is channel length, x is streamwise coordinate of the channel from the inlet center of the channel bottom wall. The heat flux $q_w(x, y)[\text{Wm}^{-2}]$ on the channel bottom is defined as:

$$q_w(x, y) = -k(T_b - T_w(x, y))/(H/2), \qquad (1)$$

where, $y\,[\text{m}]$ is spanwise coordinate of the channel, $k\,[\text{Wm}^{-1\circ}\text{C}^{-1}]$ is fluid thermal conductivity, $T_w(x, y)\,[°\text{C}]$ is measured temperature on the bottom wall, and $H\,[\text{m}]$ is fluid depth. The heat flux is directed to the bulk fluid from the bottom wall as defined in Eq. (1), so the heat flux becomes negative in this study. Thus, the net heat flux was evaluated the absolute value in this study. To evaluate how much heat is transported from the locally heated area on the free-surface to the bottom wall by the protrusions, an efficiency of the heat transport, γ can be defined as:

$$\gamma = S|q_w|/(Q_{in} - Q_{loss}), \qquad (2)$$

where, $S\,[\text{m}^2]$ is higher temperature area of $q_w < -2.00 \times 10^3\,\text{Wm}^{-2}$, $Q_{in}\,[\text{W}]$ is input power and, $Q_{loss}\,[\text{W}]$ is heat loss of the test channel. The efficiency of heat transport is evaluated as a scalar value as mentioned above.

4. Results and discussions

Fig. 3 shows the distributions of temperature rise, which is the difference between $T_w(x, y)$ and T_{in}, at the channel bottom wall for the different streamwise pitch lengths in case of N = 0.00. The high temperature rise region in case of the middle streamwise pitch length ($L_p = 0.36 \times 10^{-1}$ m) was the nearest location to the heater than other cases. It can be considered that the middle streamwise pitch length arrangement can transport high temperature fluids near the free-surface to the wall efficiently. In addition, the peak temperature rise of the distribution in case of $L_p = 0.36 \times 10^{-1}$ m showed the highest temperature rise among three L_p cases, and it was found that the higher temperature rise region was bigger than others. This means in N = 0.00 that the heat transport of the locally heated fluid on the free-surface to
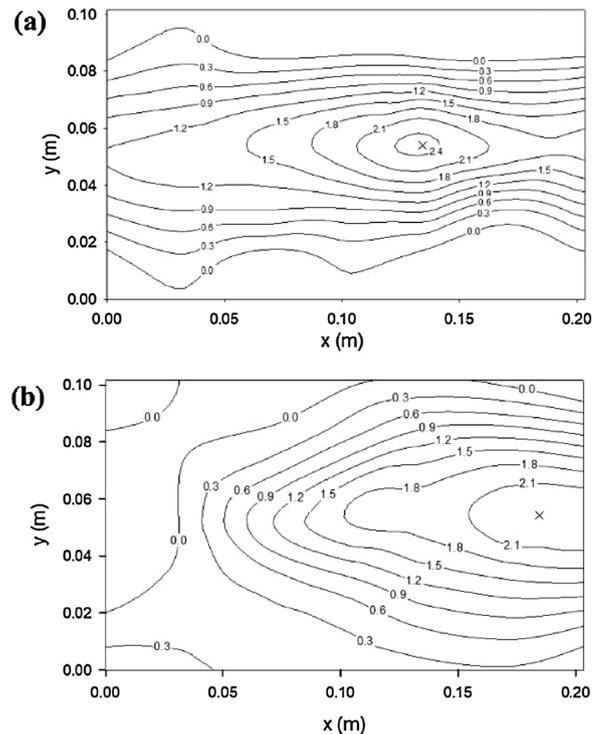

Fig. 3. Temperature rise distributions of each different L_p arrangements in case of N = 0.00 ("×" marks show the peak temperature rise location): (a) $L_p = 0.36 \times 10^{-1}$ m; Re = 5.79×10^3, (b) $L_p = 0.0480$ m; Re = 5.78×10^3.

the bottom wall for the case of the middle streamwise pitch length ($L_p = 0.36 \times 10^{-1}$ m) is larger than that of shorter ($L_p = 1.75 \times 10^{-2}$ m) or longer pitch length ($L_p = 0.48 \times 10^{-1}$ m) cases. According to the previous studies [8,9], the case of the 1.25 times longer the streamwise pitch length (middle length case) than the shortest streamwise pitch length was shown the best heat transport performance of the protrusions in the inline arrangement. Moreover, it was worse the heat transport performance in case of the 1.50 times longer the streamwise pitch length than the shortest case. In addition, the flow separation and the horseshoe vortex generated surroundings of the hemisphere on the bottom wall may have the same structure reported in the previous study [10], so it can be considered that these protrusions efficiently transport the heat from the free-surface to the bottom wall. Therefore, the thermal mixing can be enhanced by this mechanism, eventually the efficiency of heat transport can be increased.

Fig. 4 shows heat flux distributions Eq. (1) of $L_p = 0.36 \times 10^{-1}$ m in case of N = 0.00 and N = 7.92. The peak of heat flux location moved to the upstream of the channel with increase of the transverse magnetic field strength, so it can be transported localized heat near free surface to the wall with a short distance. However, the heat flux decreased with increase of the transverse magnetic field strength, it denotes the same tendency of the previous study [7], so it can be considered that the transverse magnetic field prevented thermal mixing enhancement. Comparing heat flux distributions between N = 0.00 and N = 7.92, the peak value of heat flux in case of N = 0.00 was 2.50 times higher than that of N = 7.92. Therefore, the relatively high transverse magnetic field enhanced a thermal stratification in the film flow due to the MHD force, so it prevented the heat transport. According to Molokov [11], the transverse magnetic field made flow velocity jets near the free surface of the film flow. In addition, the flow velocity of bulk fluid other than the boundary layer near the free-surface and the bottom wall is decreased by the Lorentz force. Therefore, the flow laminarization occurs under the transverse magnetic field, it is considered that this laminarization and the localized heating on the free-surface were induced
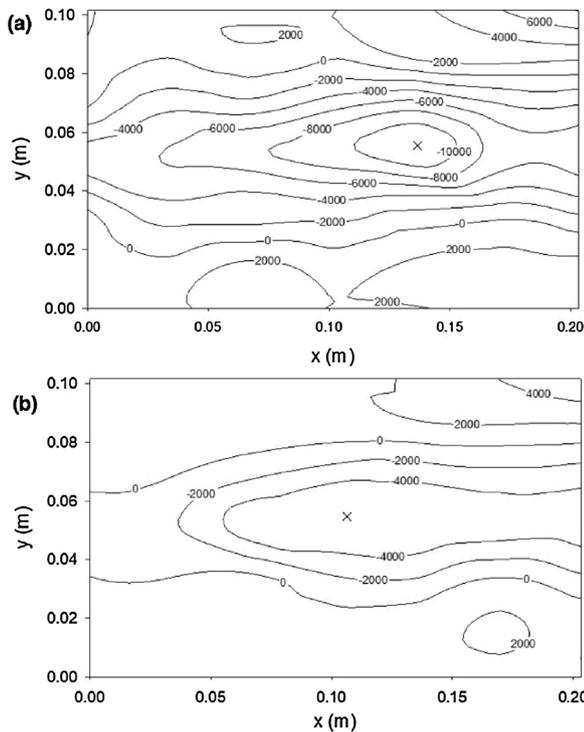
Fig. 4. Heat flux distributions of $L_p = 0.36 \times 10^{-1}$ m arrangement in case of N = 0.00, 7.92 ("×" marks show the peak of heat flux locations): (a) N = 0.00, Re = 5.79 × 10³, (b) N = 7.92, Re = 5.58 × 10³.
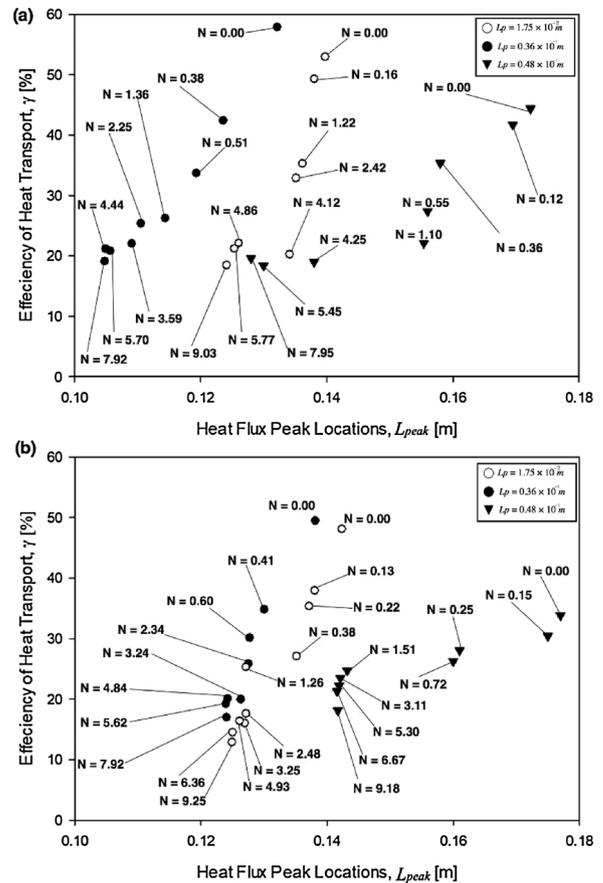

Fig. 5. Relation between efficiency of heat transport and heat flux peak locations for $L_p = 1.75 \times 10^{-2}$ m, 0.36×10^{-1} m and 0.48×10^{-1} m; (a) $Q_{flowrate} = 1.21 \times 10^{-4}$ m³ s⁻¹, (b) $Q_{flowrate} = 1.67 \times 10^{-4}$ m³ s⁻¹.

temperature stratification.

Fig. 5 shows the relationships of the heat transport efficiency and the peak heat flux location (L_{peak}) in cases of (a) $Q_{flowrate} = 1.21 \times 10^{-4}$ m³ s⁻¹ and (b) $Q_{flowrate} = 1.67 \times 10^{-4}$ m³ s⁻¹. The origin of L_{peak} is the thermocouples at the most upstream location on the bottom wall. The efficiencies decrease with increase of the transverse magnetic field strengths and converge to a certain value (γ–20.0%) at relatively high transverse magnetic field on each L_p configuration. The reason for the decrease of γ at relatively high transverse magnetic field is that the thermal mixing enhancement is decreased by suppressing the flow velocity due to the MHD effect, and the jet flow near the free surface caused by the protrusions transports the relatively high temperature fluids to the downstream, and also the heat loss increases with increase of the magnetic field. As shown in Fig. 5(a), the peak heat flux location L_{peak} for various N in case of $L_p = 0.36 \times 10^{-1}$ m at $Q_{flowrate} = 1.21 \times 10^{-4}$ m³ s⁻¹ was shortened, this means that it is possible to remove heat quickly from the bottom wall if the peak heat flux location is close to the heated surface location of the film flow, that is the shortest distance for the heat removal, and thus the inline arrangement with $L_p = 0.36 \times 10^{-1}$ m showed the best heat transport performance.

Fig. 6 shows the relationships between the heat transport efficiency γ and the streamwise pitch length L_p in cases of (a) $Q_{flowrate} = 1.21 \times 10^{-4}$ m³ s⁻¹ and (b) $Q_{flowrate} = 1.67 \times 10^{-4}$ m³ s⁻¹. The γ-plots in case of N = 0.00 were γ = 57.8, 52.9 and 44.4% for $L_p = 0.36 \times 10^{-1}$ m, 1.75×10^{-2} m and 0.48×10^{-1} m, respectively in case of $Q_{flowrate} = 1.21 \times 10^{-4}$ m³ s⁻¹. Thus, the heat transport performance in case of $L_p = 0.36 \times 10^{-1}$ m was the best on N = 0.00. The heat transport efficiency in case of MHD conditions cannot be made directly compared because N values were not same, when comparing with relatively low N value cases, the heat transport efficiency for $L_p = 1.75 \times 10^{-2}$ m showed better than any other cases under the relatively low flowrate: $Q_{flowrate} = 1.21 \times 10^{-4}$ m³ s⁻¹. The reason of this phenomenon may relate to the effect of the flow velocity decrease at the center of the bulk flow due to the MHD effect. It is because that the flow

velocity is suppressed on the center of bulk flow by relatively weak Lorentz force, and the jet flow does not generate under the relatively low strength of the transverse magnetic field [11], so it can be considered that high temperature fluids near free-surface transported to the wall, however heat transportation deterioration occurred more than in case of N = 0.00. Therefore, it is suggested that the optimized inline arrangement for the enhancement of heat transport efficiency might be different depending on the difference in the magnetic field strength and the flow conditions.

This study provided a deeper understanding of the transportation of the localized surface high heat flux from the free-surface. The experimental results suggested that in case of relatively high flow rate the inline arrangement of the hemispherical protrusions with the middle streamwise pitch length effectively transported the localized high heat flux from the free-surface to the bottom wall of the MHD liquid metal free-surface film flow under the transverse magnetic field. On the other hand, to install the relatively short streamwise pitch length showed the best heat transport performance under low magnetic field and relatively low constant flow rate. In summary, the relation of the heat transport efficiency and heat flux locations propose for installing the middle streamwise pitch length hemisphere arrangement for quickly heat removal in this study.

As for the implementation to the liquid divertor design, the optimal streamwise pitch length should be installed in the traverse magnetic field area on the divertor. The impinging cooling jets on the back-side of the wall to remove localized high heat flux from the bottom wall should be considered for this divertor design. However, there are reaming three issues to be solved: the first issue is to grasp the efficiency of heat transport of the optimum streamwise pitch length between the middle streamwise pitch 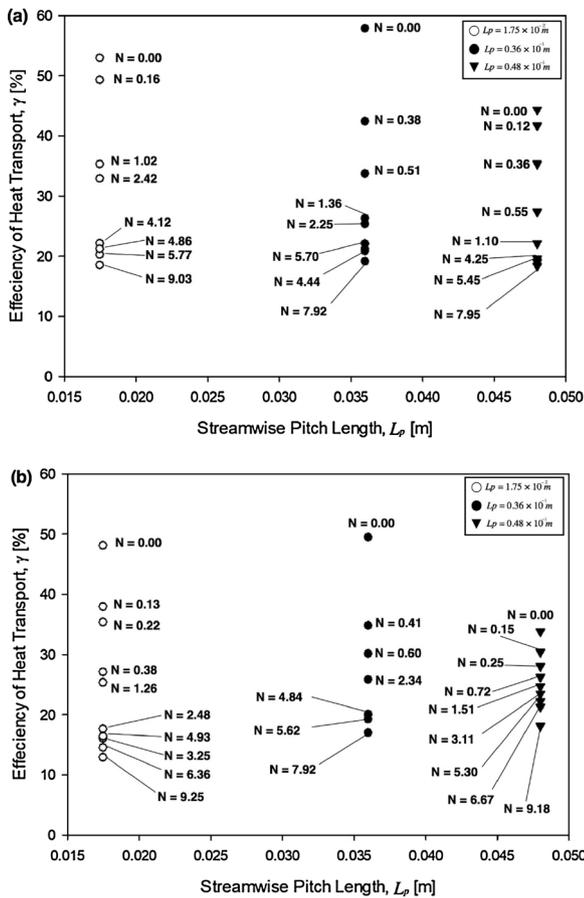length and the shortest length for finding best